Inhibition of IMPDH by Mycophenolic Acid: Dissection of Forward and Reverse Pathways Using Capillary Electrophoresis

Mark A. Fleming,* Stephen P. Chambers, Patrick R. Connelly,‡ Elmar Nimmesgern, Ted Fox, Frank J. Bruzzese, Stephen T. Hoe, John R. Fulghum, David J. Livingston, Cameron M. Stuver, Michael D. Sintchak, Keith P. Wilson, and John A. Thomson*

Vertex Pharmaceuticals Incorporated, 40 Allston Street, Cambridge, Massachusetts 02139-4211

Received March 27, 1996; Revised Manuscript Received April 19, 1996⊗

ABSTRACT: The objective of this work was to contribute to the understanding of mechanisms for IMPDH inhibition. We over-expressed hamster type II IMPDH in *Escherichia coli*, purified the protein to apparent homogeneity, and used capillary electrophoresis to quantify enzyme turnover events accompanying inhibition by mycophenolic acid (MPA). We dissected two convergent pathways leading to MPA-inhibition; a rapid "forward" pathway beginning with substrates and linked to enzyme catalysis, and a slower "reverse" pathway apparently not involving catalysis. MPA-inhibition occurred rapidly in the forward direction by interrupting the enzyme turnover cycle, after IMP and NAD^+ binding, after hydride transfer, and after NADH release. Slow inhibition, without substrate turnover, was achieved by incubating free enzyme with excess XMP and MPA. We propose that mycophenolic acid inhibits IMPDH by trapping a transient covalent product of the hydride transfer reaction (IMPDH∼XMP*) before a final hydrolysis step that precedes XMP and enzyme release in the forward reaction pathway. Understanding the ligand occupancy of the protein has also proven important for producing homogeneous, chemically defined complexes for structural studies. IMPDH samples inhibited by MPA in the forward and reverse pathways yielded similar, high-quality crystals that are currently undergoing X-ray diffraction analyses.

Inosine 5′-monophosphate dehydrogenase (IMPDH)[1] (IMP:NAD^+ oxidoreductase; EC 1.1.1.205) catalyzes the NAD^+-dependent oxidation of inosine 5′-monophosphate (IMP) to xanthosine 5′-monophosphate (XMP). This is the committed, and probably rate-limiting, step in the *de novo* pathway for guanine nucleotide biosynthesis (Crabtree & Henderson, 1971; Snyder *et al*., 1972; Jackson *et al*., 1975; Weber, 1983). IMPDH homologues identified in bacteria, protozoa, and mammals share 30%−40% sequence identity (Collart & Huberman, 1988; Natsumeda *et al*., 1990; Beck *et al*., 1994). In some mammalian species two isoforms have been identified. The human isoforms, designated types I and II, share 84% sequence identity with each other (Natsumeda *et al*., 1990) and >98% identity with their respective hamster counterparts (S. P. Chambers, unpublished). IMPDH activity is elevated in tumors, activated T-cells, and other proliferating tissues. Some studies suggest that the type I enzyme is constitutive and dominant in most cell types, whereas the type II enzyme is strongly up-regulated in actively-replicating cells (Jackson *et al*., 1975; Weber, 1983; Natsumeda *et al*., 1988; Collart & Huberman, 1990; Konno *et al*., 1991; Nagai *et al*., 1991; Collart *et al*., 1992; Nagai *et al*., 1992; Nakamura *et al*., 1992; Senda & Natsumeda, 1994). This may be an oversimplification, because Dayton *et al*. (1994) have evidence that both isoforms are similarly up-regulated in activated human T-cells. Nevertheless, many still regard IMPDH as a promising molecular target for antiparasitic, antiviral, antineoplastic, and immunosuppressive chemotherapies.

Mycophenolic acid (MPA) is a small molecule, originally identified from fungal extracts as an antimicrobial agent (Gosio, 1896) and later shown to inhibit the proliferation of cultured human lymphocytes. For reviews of MPA, see Allison and Eugui (1993) and Wu (1994). MPA is a tight-binding, uncompetitive inhibitor of IMPDH (Franklin & Cook, 1969; Synder *et al*., 1972; Lee *et al*., 1985; Verham *et al*., 1987; Hedstrom & Wang, 1990; Hager *et al*., 1995). Mycophenolate mofetil is a morpholinoethyl ester pro-drug of MPA that is being developed as an immunosuppressive agent for organ transplantation patients. It has been approved in the United States and Europe for treatment of human kidney-transplant recipients (Shaw *et al*., 1995; Sollinger *et al*., 1995). Unfortunately, early clinical findings suggest MPA has toxic side effects that may ultimately limit its use as a human therapeutic (Pichlmayr *et al*., 1995; Shaw *et al*., 1995; Sollinger *et al*., 1995). Therefore, like others [e.g., Tricot *et al*. (1990)], we are attempting to develop new IMPDH inhibitors that will improve upon MPA's immunosuppressive properties yet circumvent its toxic effects.

Native IMPDH's from all known species appear to exist as homotetramers of 56−58 kDa gene products, or protomers

* Authors to whom correspondence should be addressed. Tel: (617) 576-3111. FAX: (617) 576-2109. E-mail: Fleming@vpharm.com and Thomson@vpharm.com.

‡ Present address: Groton School, Farmers Row, Groton, MA 01450.

⊗ Abstract published in *Advance ACS Abstracts,* May 15, 1996.

[1] Abbreviations: IMPDH, inosine 5′-monophosphate dehydrogenase; IMP, inosine 5′-monophosphate; XMP, xanthosine 5′-monophosphate; NAD^+, β-nicotinamide adenine dinucleotide; NADH, β-nicotinamide adenine dinucleotide reduced form; MPA, mycophenolic acid; CZE, capillary zone electrophoresis; CHO, Chinese hamster ovary; PCR, polymerase chain reaction; IPTG, isopropyl β-D-thiogalactoside; EDTA, ethylenediaminetetraacetic acid; PMSF, phenylmethylsulfonyl fluoride; NADH-DH, NADH-dehydrogenase; SDS−PAGE, sodium dodecyl sulfate polyacrylamide gel electrophoresis; DTT, DL-dithiothreitol; UV, ultraviolet; MeP, 1-methyl-2-pyrrolidinone; PEG, polyethylene glycol; EICAR, 5-ethynyl-1-β-D-ribofuranosylimidazole-4-carboxamide. For specific nomenclature used for enzyme complexes, refer to the legend to Figure 5.

S0006-2960(96)00741-6 CCC: $12.00

(Gilbert *et al*., 1979; Okada *et al*., 1983; Hupe *et al*., 1986; Verham *et al*., 1987; Collart & Huberman, 1988; Natsumeda *et al*., 1990; Carr *et al*., 1993; Pugh & Skibo, 1993; Beck *et al*., 1994). X-ray crystallographic studies of free IMPDH from *Tritrichomonas foetus* are underway (Whitby *et al*., 1995), but no high-resolution structural information is yet available for IMPDH in any form. Studies of IMPDH catalysis and inactivation are numerous. The enzymatic mechanism appears to follow an ordered bi-bi reaction sequence, with IMP binding first and NAD^+ second, forming an IMPDH−IMP−NAD ternary complex. Following hydride transfer from IMP to NAD^+, NADH is released and then XMP (Brox & Hampton, 1968; Holmes *et al*., 1974; Yamada *et al*., 1988; Hedstrom & Wang, 1990; Carr *et al*., 1993). Several reports suggest the formation of a covalent intermediate between IMP and IMPDH during catalysis (Hedstrom & Wang, 1990; Antonino *et al*., 1994; Antonino & Wu, 1994; Huete-Perez *et al*., 1995). However, the precise chemical mechanism for IMP to XMP conversion is yet to be demonstrated.

There are also unresolved questions concerning MPA-inhibition. K_i values of 9−14 μM (versus IMP and NAD^+) are reported for MPA-inhibition of *T. foetus* IMPDH (Verham *et al*., 1987; Hedstrom & Wang, 1990; Huete-Perez *et al*., 1995). Reported K_i values for human type II IMPDH are 6−10 nM (Carr *et al*., 1993; Hager *et al*., 1995), and estimates for the human type I enzyme vary from 11 nM (Hager *et al*., 1995) to 33−37 nM (Carr *et al*., 1993). No time-dependence has been observed for MPA-inhibition of the human enzymes (Wu, 1994). The uncompetitive nature suggests that MPA-inhibition occurs after both substrates have associated with the enzyme (Hedstrom & Wang, 1990; Wu, 1994; Hager *et al*., 1995; Huete-Perez *et al*., 1995). Wu (1994) has suggested MPA inhibits by binding to an IMPDH−IMP−NAD ternary complex or an IMPDH−XMP binary complex. Studying multiple-inhibitor effects on the *T. foetus* enzyme, Hedstrom and Wang (1990) concluded that MPA is uncompetitive with IMP (K_{ii} = 14 μM) and noncompetitive with NAD^+ (K_{is} = 20 μM, K_{ii} = 14 μM). The authors proposed that MPA binds to the nicotinamide subsite of the NAD^+ binding site but that the drug does not simply stabilize the final IMPDH−XMP complex. They suggested two alternative mechanistic explanations. One is a non-covalent, general acid−base scheme, involving XMP tautomerization prior to release. The other proposes that a covalent enzyme−XMP adduct is generated after the hydride transfer steps. They predicted that this adduct would require hydrolysis for XMP release, a step that would be essentially irreversible.

EXPERIMENTAL PROCEDURES

Materials. Highest grade available IMP (free acid), NAD^+, NADH (disodium salt), and XMP (sodium salt) were purchased from the Sigma Chemical Company. MPA was obtained from Calbiochem Corporation. Separate CZE analyses revealed a single peak for each ligand (see below).

Expression of Recombinant IMPDH in E. coli. Hamster (*Cricetulus griseus*) type II IMPDH cDNA was isolated from a commercial Chinese hamster ovary (CHO) cDNA library (Clontech). A 1545 base pair fragment was produced by PCR amplification using cDNA primers (5′-ATGGCCGACTACCTGATTAGTGGG-3′ and 5′-TCAGAAAAGCCGCTTCTCATACGA-3′, respectively) corresponding to the N- and C-termini of the CHO IMPDH sequence (Collart & Huberman, 1988). When sequenced, the fragment was confirmed as the CHO IMPDH gene. We introduced an *Nde*I site (CATATG) before the AUG translation initiation codon of the CHO IMPDH gene, and an *Xba*I site distal to its 3′ termination. This enabled insertion of the IMPDH gene into pFlag I (IBI), producing the expression vector designated pchoIMPDH(II). Recombinant hamster type II IMPDH was expressed in H712 (gua B^-), a mutant *E. coli* strain deficient in IMPDH (Nijkamp & Haan, 1967). Cells were grown at 37 °C in a 10 L fermentor, on complex media supplemented with 1 mM IPTG allowing constitutive expression. Cells were harvested after 14 h, flash frozen, and stored at −70 °C prior to purification.

Protein Purification. The recombinant IMPDH was purified by modifying previous methods (Gilbert *et al*., 1979; Ikegami *et al*., 1987) as follows: All steps were done at about 4 °C. Typically 100 g of *E. coli* cell paste was thawed in 5 volumes of buffer A (50 mM Tris-HCl, 300 mM KCl, 2 mM EDTA, 10 mM β-mercaptoethanol, 1.5 M urea, pH 8.0 at 4 °C). Protease inhibitors were added (0.2 mM PMSF and 1 μg/mL each of pepstatin, leupeptin, and E-64), and the cells were lysed in a microfluidizer. Cellular debris was removed by centrifugation at 45 000*g* for 40 min. Crystalline ammonium sulfate was added slowly to the stirred supernatant, to a final concentration of 25 g per 100 mL of supernatant. The solution was allowed to stabilize for 1 h, whereupon the insoluble protein was harvested by centrifugation, as above. The precipitate was resuspended in buffer B (50 mM Tris-HCl, 300 mM KCl, 2 mM EDTA, 10 mM β-mercaptoethanol, 10% glycerol, pH 8.0 at 4 °C). Aliquots were stored at −70 °C prior to loading (20% at a time) onto a 5 × 12.5 cm column of IMP-Sepharose, prepared from epoxy-activated Sepharose (Pharmacia) essentially as described (Gilbert *et al*., 1979). The affinity column was washed with ≥4 column volumes of buffer B, before eluting the enzyme with the same buffer containing 10 mM IMP (pH readjusted to 8.0 at 4 °C, with KOH). Affinity purified IMPDH appeared to be >95% pure, as judged by SDS−PAGE, but analytical size-exclusion chromatography and light-scattering measurements showed about 30% of the protein was highly-aggregated. The protein was concentrated by ultrafiltration to about 5 mg/mL (50 mL) and then fractionated on a Sepharcyl S-300 (Pharmacia) size-exclusion column (5 × 90 cm, eluting at 3 mL/min in buffer B). This step removed virtually all of the non-IMPDH contaminants and aggregated IMPDH, and most of the IMP used to elute the affinity matrix. Aggregated IMPDH did not reappear upon further concentration, but some purified samples still contained small amounts of IMP. The latter was removed by exhaustive dialysis under N_2, when necessary.

Using the above expression system we found that hamster IMPDH II represented about 10% of the soluble protein from the bacterial extracts. Not surprisingly, the IMPDH specific activity increased only by a factor of about 10 during the entire purification. However, the bacterial extracts also contained variable levels of NADH-dehydrogenase (NADH-DH)[2] activity. In the early stages of the purification the NADH-DH activity obscured IMPDH activity when the NADH formation was monitored directly. Therefore, prior to the affinity chromatography elution, IMPDH activity was determined (assay buffer consisting of buffer B with 0.3 mM

IMP and 0.25 mM NAD^+) by taking the change in UV absorption at 290 nm as a measure of XMP production (Brox & Hampton, 1968). For pure IMPDH samples, we monitored the increase in UV absorption at 340 nm as a direct measurement of NADH formation (same assay buffer as above). Typically, a single passage through the IMP-affinity and size-exclusion procedures reduced the starting NADH-DH activity by $\geq 10^3$-fold. Analyses of purified IMPDH samples at the high protein concentrations used for the CZE separations (>9 mg/mL) usually showed undetectable NADH-DH activity. When the residual activity was sufficient to complicate CZE analyses, it was reduced to undetectable levels by repetition of the above-mentioned chromatographic procedures. SDS−PAGE and N-terminal sequence analysis indicated that the IMPDH samples were >99% pure.

Enzyme kinetic parameters for the recombinant hamster protein were measured at 37 °C in 100 mM potassium phosphate, 0.5 mM EDTA, 2 mM DTT, pH 8.0. The observed k_{cat} for the pure protein was 0.76 s^{-1} ([E] = 85 nM). The K_m values for IMP and NAD^+ and were 22 and 37 μM, respectively ([E] = 85 nM). The observed K_{ii} for MPA (with respect to NAD^+) was 11 nM (±10%) ([E] = 20 nM). We observed that MPA is uncompetitive toward both substrates. IMPDH concentrations were determined by UV spectroscopy, using a specific molar absorption coefficient (A_{278}) of 23 800 M^{-1} cm^{-1}, expressed relative to IMPDH protomer concentration.

Capillary Zone Electrophoresis. Free-solution capillary zone electrophoresis (CZE) experiments were performed on a Hewlett Packard 3DCE system with a diode-array UV-absorption detector, using Hewlett Packard fused silica capillaries (50 μm i.d. × 56 cm effective length) with extended light paths. The electrolyte was 50 mM sodium borate, pH 9.5−9.8, optimized for reproducibility of retention times for each new capillary. Samples were loaded at constant [time × pressure] (nominally 5 s at 50 mbar). Separations were run at +30 000 V, which was ramped linearly from 0 V over the first 30 s of each separation. Capillaries were maintained at 30 °C and were washed extensively (cycling 8 M urea, 1 M NaOH, and electrolyte buffer) between analyses. Electropherograms were generated by recording the UV absorbance of eluents at 200 nm. UV-absorption spectra (200−400 nm) were also stored throughout the separations to further assist identification of components. IMPDH solutions were prepared in buffer B, with or without MPA and substrates.

Protein Crystallization. Typically we inhibited the protein via the forward pathway (see below). 100 mg of pure free IMPDH (2−4 mg/mL) was placed in a stirred ultrafiltration cell with a 30 kDa MW cutoff membrane. A stock of 100 mM MPA in 1-methyl-2-pyrrolidinone (MeP) was added to a final concentration of 2 mM MPA. IMP and NAD^+ were then added in a 2-fold molar excess over IMPDH protomers, and the solution was allowed to equilibrate at room temperature for 30 min. The complex was concentrated and exchanged into fresh buffer B containing 2 mM MPA, until no IMP, NAD^+, or NADH was detectable by CZE ($\geq 10^3$ dilution of each). For inhibition via the reverse pathway

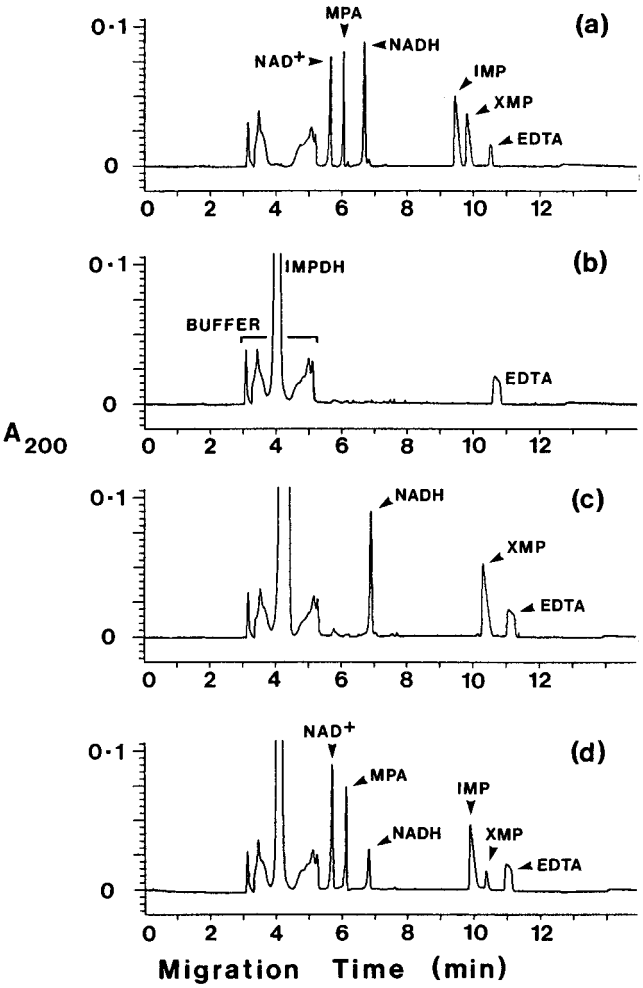

FIGURE 1: CZE electropherograms of IMPDH and/or ligand mixtures. (a) Standard mixture of NAD^+, MPA, NADH, IMP, and XMP, all at 400 μM, in buffer B; (b) 200 μM IMPDH in buffer B; (c) 200 μM IMPDH in buffer B, 500 μM IMP and 500 μM NAD^+, incubated at 22 °C for 1 h prior to CZE analysis; (d) 200 μM IMPDH in buffer B, 500 μM MPA, 500 μM IMP, and 500 μM NAD^+, incubated at 22 °C for 1 h prior to CZE analysis.

we incubated 25 μM free IMPDH with 1 mM XMP and MPA for 24 h at 22 °C and then exchanged the samples into buffer B containing 2 mM MPA. Fully inhibited complexes were finally concentrated to 15−60 mg/mL, harvested, and centrifuged at 45 000*g* for 20 min at 4 °C. 100 μL aliquots were stored at −70 °C until use in crystallization experiments. Using hanging-drop vapor diffusion methods, large crystals (0.2 mm × 0.2 mm × 1.8 mm) were obtained within 48−72 h when 4 μL of protein (20 mg/mL in buffer B) was mixed with 2 μL of reservoir [10% PEG 6000, 1 M LiCl, 100 mM MES, 5.4% MeP (v/v), 36 mM β-mercaptoethanol, pH 5.9] and allowed to equilibrate over the reservoir solution at 22 °C. The crystals belonged to space group *P*4, with unit cell dimensions $a = b = 110.6$ Å, $c = 111.0$ Å and angles $\alpha = \beta = \gamma = 90°$. There were two IMPDH protomers per asymmetric unit.

RESULTS AND DISCUSSION

We began by developing a CZE separation of NAD^+, NADH, IMP, XMP, MPA, and IMPDH. Each peak in the CZE electropherograms was identified by monitoring the migration times and UV-absorption spectra for each component in simpler mixes. Figure 1a shows a typical

[2] We did not purify or characterize the "NADH-dehydrogenase" contaminant to establish its formal dehydrogenase/oxidase/oxidoreductase identity. For the purpose of discussion, the contaminating activity was simply abbreviated "NADH-DH".

separation of the ligands all at 400 μM. Figure 1b, representing a typical separation of unliganded IMPDH (200 μM) in sample analysis buffer, shows that the protein and buffer components were well-resolved from all relevant ligands. Upon incubating 200 μM IMPDH with both substrates at 500 μM the reaction proceeded to completion within an hour at 22 °C (Figure 1c), with all of the NAD^+ and IMP converted to NADH and XMP, respectively. Essentially identical results were obtained when the enzyme incubation period was reduced to 5 min. When repeated with 500 μM MPA in the incubation mixture (Figure 1d) the recovery of each substrate closely matched the initial excess of substrates over enzyme protomers ([S] − [E] = 300 μM). The amount of recovered NADH remained slightly below the enzyme protomer concentration (200 μM) with somewhat less XMP being recovered. These results imply that essentially complete MPA-inhibition occurred during a partial enzyme turnover cycle, after both substrates had bound and after hydride transfer.

To quantify the stoichiometry of catalysis-dependent MPA-inhibition more precisely, we made stock solutions of {IMPDH + MPA} and {IMP + NAD^+} (equimolar substrates). Parallel dilution gave a range of samples with different substrate concentrations but constant enzyme and inhibitor concentrations. The samples were incubated for ≥1 h at 22 °C to allow complete equilibrium and then subjected to CZE. Consistent sampling was ensured by loading at constant [time × pressure] with a common buffer system. Ligand recovery (CZE peak area) was converted to the apparent concentration present in the loaded sample, using calibration curves derived from standard ligand mixtures. When the same CZE capillary was used, quantification was linear for each ligand ($r > 0.99$; average of $n = 4$ analyses) between 50 and 1000 μM, with less than 10% variation between analyses. Thus, all recovery data were within the linear response range for each ligand. It was also established that, with the exception of MPA and XMP, each ligand was recovered quantitatively from the IMPDH-containing samples (see below). Figure 2 summarizes the recovery of substrates from samples containing 200 μM IMPDH and 500 μM MPA, and initial substrate concentrations of 50−1000 μM. When the initial substrate concentrations were below the IMPDH protomer concentration, only NADH and XMP were recovered, and product formation appeared to be approximately stoichiometric to the added substrates. Above 200 μM initial IMP/NAD^+ concentrations, the recovery of NADH and XMP remained essentially constant. Recovery of NADH was about 95% of the IMPDH protomer concentration, and XMP recovery was about 80%. At substrate concentrations above the enzyme concentration, the additional substrates were recovered quantitatively as the IMP/NAD^+ levels increased linearly ($r > 0.99$) up to 1000 μM ([S]/[E] = 5). These findings suggest a 1:1:1 stoichiometric relationship between enzyme concentration, substrate turnover, and enzyme inhibition, when MPA and substrates are in excess.

At this point it was unclear whether MPA inhibits IMPDH with NADH and XMP still bound or following the release of product(s). We could not distinguish directly between protein-bound and free ligands using CZE separations, so some samples were examined after dialysis and ultrafiltration. First, a 200 μM enzyme solution was prepared in the presence of 500 μM MPA, 400 μM IMP, and NAD^+. From

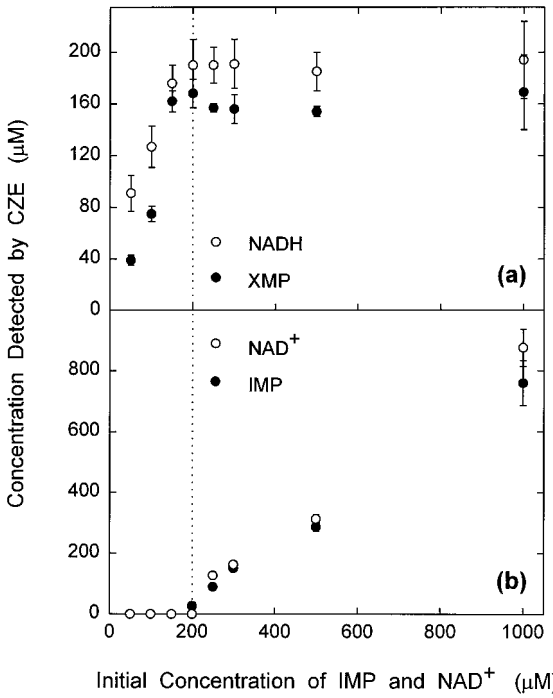

FIGURE 2: Stoichiometry of catalysis-dependent MPA-inhibition of IMPDH. Quantification of CZE analyses of samples containing 200 μM IMPDH and 500 μM MPA in buffer B, incubated with different (equimolar) IMP and NAD^+ concentrations for 1 h at 22 °C prior to CZE: (a) recovery of XMP (closed circles) and NADH (open circles); (b) recovery of IMP (closed circles) and NAD^+ (open circles). The data points (see text for details) represent the averages of triplicate assays, and the error bars define the standard deviations. The dotted vertical line shows the IMPDH protomer concentration.

our earlier results we expected half of the substrates to be converted to products and leave equimolar (200 μM) IMPDH, NAD^+, IMP, NADH, and XMP. Half of this solution (200 μL) was placed in a 30 kDa (MW cutoff) ultrafiltration spin-concentrator (Microcon 30; Amicon Inc.), and the sample was centrifuged at 22 °C and 10 000*g*. The first 25% of the solution was discarded after it passed through the membrane, and the next 25% was collected for analysis as "filtrate". The retentate and filtrate were then analyzed by CZE (Figure 3a,b, respectively). The remainder of the original incubation mixture was dialyzed exhaustively against 500 μM MPA in buffer (10 kDa MW cutoff Slide-A-Lyzer cassette; Pierce), to remove any free ligands while maintaining inhibition. This sample was then also analyzed by CZE (Figure 3c). A slight decrease in the NADH peak recovered from the ultrafiltration filtrate suggests that some losses occurred, probably via nonspecific membrane binding. Nevertheless, the separations clearly show NADH was not present in the dialyzed sample and that it passed through the ultrafiltration and dialysis membranes along with the free IMP and NAD^+. XMP was undetectable in the ultrafiltration filtrate, whereas it was recovered from the retentate and the dialyzed sample. We conclude that only MPA and some form of XMP (XMP or a chemical intermediate between IMP and XMP) was bound in the inhibited complex. Thus, MPA-inhibition traps either a non-covalent IMPDH−XMP complex (IMPDH·XMP)[3] or a water-labile, covalent precursor (IMPDH∼XMP*).[3]

[3] For our definition of symbols used to describe covalent and non-covalent complexes, refer to the legend to Figure 5.

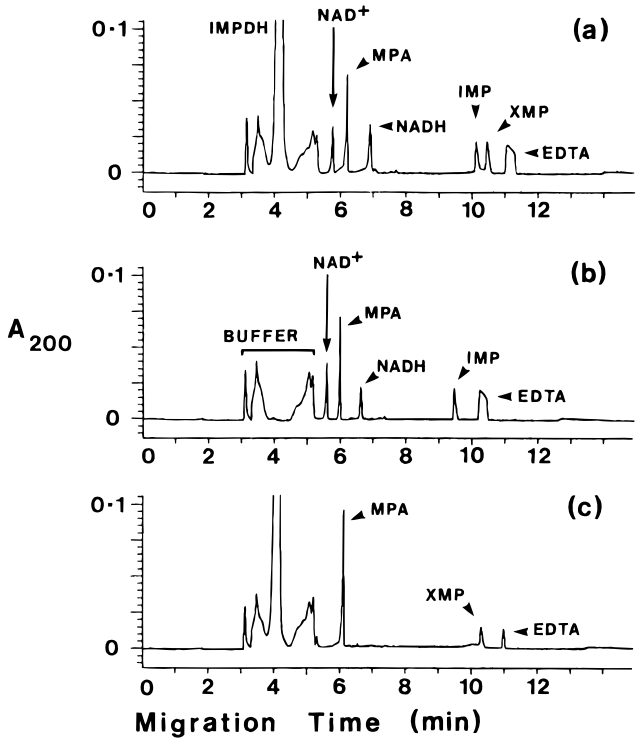

FIGURE 3: Separation of bound and unbound ligands from MPA-inhibited IMPDH. CZE electropherograms of ultrafiltered or dialyzed fractions from a 200 μM IMPDH solution, initially prepared in the presence of 500 μM MPA, 400 μM IMP, and 400 μM NAD^+. Panels: (a) ultrafiltration retentate, (b) ultrafiltration filtrate, and (c) sample dialyzed exhaustively against 500 μM MPA buffer (see text for details).

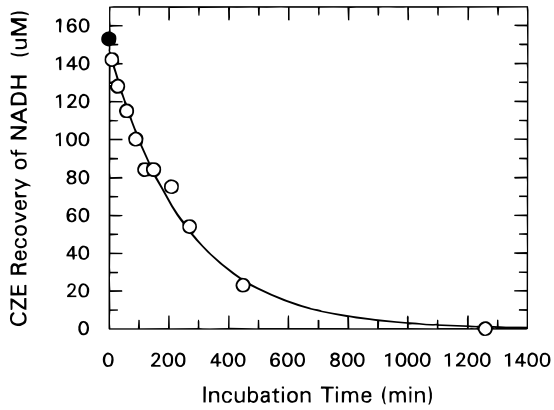

FIGURE 4: Rate of catalysis-independent inhibition of IMPDH. Aliquots were prepared containing IMPDH (182 μM in buffer B) with 1.1 mM XMP and 1.1 mM MPA. The samples were incubated at 22 °C for times $t = 0-1260$ min, before diluting them 10% with 5 mM IMP and NAD^+. Final concentrations: 164 μM IMPDH, 1 mM XMP, 1 mM MPA, 0.5 mM IMP, and 0.5 mM NAD^+. The samples were allowed to react for >30 min prior measuring product generation by CZE (see text for details). Recovery is plotted (open circles) versus the initial substrate-deficient incubation period (t). The NADH recovery at $t = 0$ (closed circle) was determined in a sample incubation for 1 min at 22 °C with the same concentration of MPA but no XMP.

The substoichiometric recovery of XMP in the dialyzed sample was accounted for, only in part, by a decrease (~10%) in the protein concentration. CZE analyses usually gave subquantitative recovery (50%−100%) of MPA and XMP from inhibited complexes; more so for samples at higher protein concentrations (see Figure 2; other data not shown). This indicates partial dissociation during the separations, irrespective of what chemical species were present in the original inhibited samples. Because the separations were performed in aqueous borate buffer (pH 9.5) we could not use CZE directly to distinguish between a non-covalent complex (MPA·IMPDH·XMP) and a water-labile covalent complex (MPA·IMPDH~XMP*). Therefore, we sought evidence for either by attempting to form inhibited complexes in the backward direction, beginning with free IMPDH, MPA, and XMP.

We incubated IMPDH with a >6-fold molar-excess of XMP and MPA and no substrates. At times $t = 0-1260$ min, excess IMP and NAD^+ (>2.7-fold final excess) was added and the samples were examined by CZE (see legend to Figure 4 for details). From our earlier studies, we predicted that protein remaining uninhibited during the initial incubation period would rapidly convert a stoichiometric amount of substrate and then become inhibited by the excess MPA, whereas protein inhibited during the initial incubation period would remain unable to convert substrates. Figure 4 shows the decrease in NADH recovered from a sample prepared and analyzed using this approach. For these experiments, the final protein concentration was 164 μM prior to CZE analysis. The NADH recovery was 154 μM at $t = 0$ min and decreased exponentially with incubation time, becoming undetectable at 21 h. This demonstrates the slow but complete inhibition of IMPDH upon prolonged incubation with XMP and MPA. Thus, there appear to be distinct "catalysis-dependent" (forward) and "catalysis-independent" (reverse) pathways for MPA-inhibition. We also found that stoichiometric, catalysis-independent inhibition only occurred when all three components were incubated together. No decrease in NADH recovery was seen when MPA was excluded from the prolonged-incubation mixture but added 1−2 min prior to substrate addition. Even at 21 h, the NADH recovered from this sample (157 μM, or 103% of the zero-time value) was almost identical to the protein concentration (164 μM). This shows that the enzyme was not strongly inhibited during prolonged incubation with XMP, yet it remained fully inhibitable by the catalysis-dependent pathway. Essentially the same was seen when either protein or XMP was omitted from the initial incubation but then added 1−2 min prior to substrate addition. The NADH recoveries after 21 h were 116% and 112% of the zero-time values, respectively, when XMP or protein were omitted during the long incubation. When IMPDH was incubated with excess XMP, but no MPA added at any stage, the enzyme remained capable of many substrate turnover cycles, with no evidence for complete inactivation at $t =$ 1260 min. Presumably, product-inhibition by XMP ($K_i \sim$ 100 μM) was too weak, at the modest XMP molar excess, for us to detect substoichiometric inhibition with our CZE methods.

In Figure 5 we summarize our inhibition studies in the context of the known IMPDH-catalyzed reaction sequence. Although many of the steps in this scheme are complex and reversible, the enzyme catalysis mechanism, up to NADH release, is simplified and depicts only the forward direction. Our main focus was on the mode of MPA binding and inhibition, and we made no attempt to dissect possible cooperative behavior of IMPDH protomers. Obviously, our analyses were performed at supraphysiological enzyme concentrations. This enabled us to characterize single enzyme turnover events in a simple, direct manner.

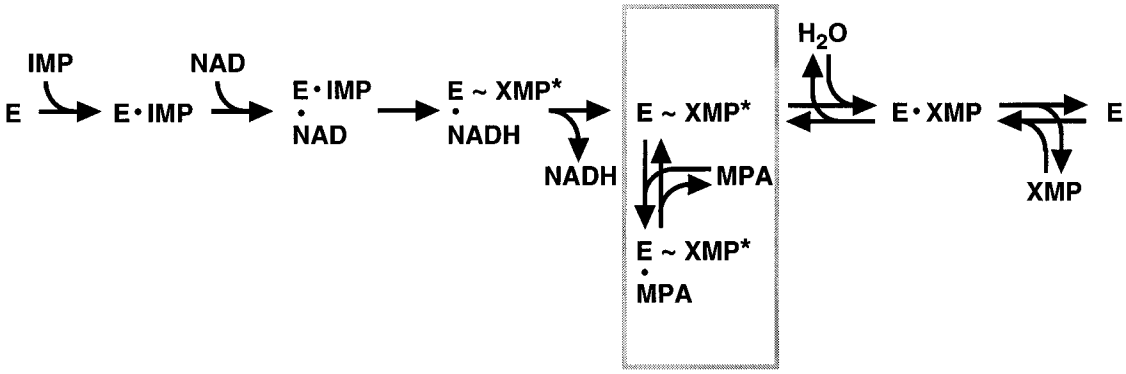

FIGURE 5: Reaction and inhibition scheme for IMPDH and MPA. Symbols: "E" denotes free enzyme (IMPDH); "E·Z" denotes non-covalent binding of ligand "Z" (IMP, NAD^+, NADH, or XMP) to enzyme; "E∼IMP" indicates the formation of a putative covalent bond between the IMPDH active site cysteine (residue 331 in human and hamster type II enzymes) and the C-2 of the purine ring of IMP. "E∼XMP*" represents a chemical intermediate between IMP and XMP covalently bound to the enzyme. This putative transient complex is generated after hydride transfer from IMP to NAD^+ but before the final hydrolysis step that precedes XMP and free protein release in the forward reaction pathway. In this reaction scheme IMP binds first, followed by NAD^+, yielding the ternary complex (IMP·E·NAD^+). A covalent bond is formed between the enzyme and IMP, and hydride transfer from IMP to NAD^+ results. The data of Huete-Perez *et al*. (1995) suggest the putative covalent bond forms after binding of NAD^+. Later in the scheme, NADH is released and XMP is generated through hydrolysis of the covalent E∼XMP* bond. In the last step of the reaction, the product XMP is released and the free enzyme is reformed. We propose that MPA binds to IMPDH with an XMP precursor still covalently attached (IMPDH∼XMP*), leading to the formation of the inhibited ternary complex (MPA·E∼XMP*). Thus, the shaded region represents our model for the biologically relevant inhibitory equilibrium between MPA and IMPDH.

We have shown that essentially complete MPA-inhibition occurs rapidly in the forward direction, during one partial enzyme turnover cycle, or slowly in the backward direction. Catalysis-dependent inhibition occurred too quickly for us to characterize the kinetics using CZE. Nevertheless, a precise 1:1:1 stoichiometric relationship between IMPDH protomer concentration, substrate turnover, and MPA-inhibition was demonstrated, so all protomers appeared to be catalytically active and MPA-inhibitable. Catalysis-dependent inhibition occurred after IMP and NAD^+ binding, after the hydride transfer reactions, and after release of NADH, leaving only MPA and some form of XMP in the inhibited complex. We lack formal proof that the forward and reverse pathways lead to the same inhibited species. However, after incubation with excess MPA and XMP, the IMPDH remaining active was rapidly inhibited, in a catalysis-dependent manner, by addition of excess substrates. Furthermore, the reverse complex was also analyzed after ultrafiltration separation of free and bound ligands (analogous to the results in Figure 3). Just as in the earlier experiments (Figure 3) these analyses indicated that the reverse complex contained some bound form of XMP. Finally, complexes formed by the forward and reverse pathways yielded ostensibly identical crystals (see below). Therefore, we suggest that our results are consistent with convergent pathways. We are seeking confirmatory evidence for this by examining the concentration dependence of the two pathways and comparing the physical properties of the inhibited species generated in both directions.

No one has shown evidence for IMPDH-catalyzed conversion of XMP and NADH (products) to IMP and NAD^+ (substrates), so the enzyme-catalyzed reaction is ostensibly irreversible (Hedstrom & Wang, 1990). A number of studies have characterized the inhibition of IMPDH by XMP. There appears to be no time-dependence, but XMP-inhibition is weak. Reported K_i's for XMP are typically around 100 μM for a number of different species of IMPDH (Brox & Hampton, 1968; Yamada *et al*., 1988; Carr *et al*., 1993; Pugh & Skibo, 1993), and Hedstrom and Wang (1990) reported that XMP has K_i values of ∼11 μM versus IMP and ∼660 μM versus NAD^+, for the *T. foetus* enzyme. We now show direct evidence that rapid association of XMP with IMPDH is not sufficient to generate a species that is stoichiometrically inhibited by MPA. These findings substantiate the contention that MPA does not simply stabilize the final IMPDH·XMP complex (Hedstrom & Wang, 1990).

Hedstrom and Wang (1990) proposed two alternative mechanisms for IMPDH catalysis. One is a non-covalent, general acid−base scheme, involving water addition and then XMP tautomerization prior to release. The other proposes that a covalent enzyme−XMP adduct is generated after the hydride transfer steps. They suggest that the covalent alternative would require hydrolysis for XMP release and that this step would be essentially irreversible. We favor the latter explanation and suggest that MPA-inhibition occurs in the forward direction by forming a stable MPA·IMPDH∼XMP* ternary complex, before the final hydrolysis step that leads to XMP and enzyme release. We propose the following explanation for the reverse inactivation pathway: In aqueous environments the equilibrium between IMPDH∼XMP* and IMPDH·XMP strongly favors the latter. (This may help explain why it is difficult to demonstrate catalysis in the reverse direction.) When we incubated IMPDH with both MPA and XMP in excess (Figure 4), MPA bound most of the IMPDH∼XMP* soon after it formed. With the constant sequestering of IMPDH∼XMP* by MPA, the IMPDH·XMP levels eventually became exhausted, leaving virtually all of the protein in the inhibited state (MPA·IMPDH∼XMP*). The overall catalysis-independent inactivation process was well-described by a single-exponential decay model (Figure 4; solid line connecting data), giving an apparent, pseudo-first-order inactivation rate (with respect to IMPDH protomer concentration) of 0.0039 ± 0.0002 min^{-1} (k_{obs}) and an enzyme half-life of 178 min ($t_{1/2}$). We have preliminary data showing that solvent pH and temperature, and perhaps D_2O/H_2O solvent ratios, affect this catalysis-independent inactivation rate and half-life (data not shown). These observations would be consistent with weak binding of XMP and IMPDH (reported $K_i \approx 10-100$ μM, see above), tight-binding of MPA and IMPDH∼XMP*

($K_{ii} \approx 11$ nM), and inhibition ultimately limited by the rate- and equilibrium constants governing the interconversion of IMPDH·XMP and IMPDH∼XMP*, under the experimental conditions used.

We cannot rule out a tight MPA·IMPDH·XMP complex that forms slowly without catalysis. A bound XMP tautomerization (Hedstrom & Wang, 1990) would be one such possibility, and similar explanation of our data might be made based on the XMP tautomerization equilibrium. However, catalysis-independent inhibition requires prolonged incubation of XMP with enzyme and MPA together, so this would require MPA- and enzyme-assisted tautomerization. Time-dependent enzyme conformational changes, occurring rapidly with catalysis and slowly without catalysis, could also limit the rate of MPA-inhibition. In other studies, we have used *in vitro* proteolysis and circular dichroism analyses to obtain evidence for ligand-induced conformational changes in IMPDH. The changes appear to be rapid and only subtle, but we still cannot discount such effects. Finally, our present studies do not exclude weak MPA binding and inhibition at other points along the scheme shown in Figure 5. This has already been suggested (Hedstrom & Wang, 1990), and we have additional calorimetric evidence that it does occur (P. R. Connelly, unpublished results). However, our current studies have identified a putative covalent reaction intermediate (IMPDH∼XMP*) that is strongly inhibited by MPA.

There is already much evidence suggesting the generation of covalent intermediates in IMPDH reaction and/or inactivation pathways. EICAR-monophosphate, an irreversible IMPDH inactivator, apparently binds covalently to the active site cysteine (Cys 305)[4] of *E. coli* IMPDH (Wang *et al*., 1996). Antonino and Wu (1994) characterized the hydrolytic dehalogenation of 2-halo-IMP by IMPDH occurring in the absence of NAD^+. The authors discussed possible covalent and non-covalent mechanisms, but their data could not differentiate between the two. Other studies, characterizing the inactivation of IMPDH by 6-chloro-IMP, have provided data consistent with a covalent mechanism (Brox & Hampton, 1968; Antonino *et al*., 1994). Perhaps the most direct evidence for a covalent intermediate comes from the trapping and identification of a stable complex between radiolabeled IMP and Cys 319[4] of *T. foetus* IMPDH (Huete-Perez *et al*., 1995). This complex only formed in the presence of NAD^+, suggesting that it represented a specific IMP−enzyme complex, relevant to the reaction mechanism.

During the final preparation of this manuscript a relevant report by Link and Straub (1996) also appeared. These authors used peptide mapping and mass-spectral analyses to show that MPA probably interrupts the normal turnover cycle of human IMPDH II by trapping a covalent complex of IMPDH and a transient intermediate between IMP and XMP. Thus, using different methodology, they proposed a kinetic scheme for MPA inhibition that is similar to the one we deduced from CZE studies (Figure 5). Link and Straub also showed evidence that the covalent adduct formed during a normal, uninterrupted enzyme turnover cycle (i.e., without MPA), but their studies did not enable identification of a reverse inhibition pathway.

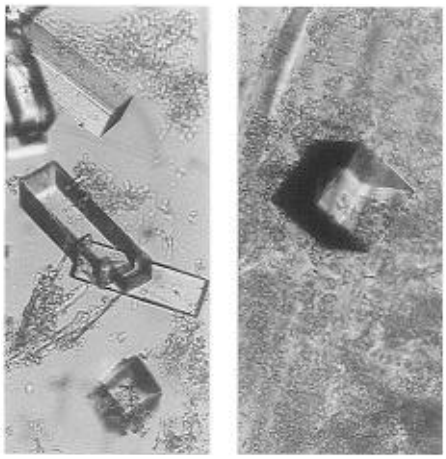

FIGURE 6: MPA-inhibited IMPDH crystals. Photographs of MPA-inhibited hamster type II IMPDH crystals: (a) complex obtained via forward inhibition, (b) complex obtained via reverse inhibition. Crystals from both pathways appeared essentially identical (see text for details).

Formal demonstration of the chemical mechanisms for IMPDH catalysis, and inactivation by MPA, will probably benefit from direct high-resolution structural analyses. In this regard, our present studies have also proven valuable. In fact, these studies were initiated because of difficulties experienced in attempting to grow high-resolution cyrstals for X-ray studies. Using CZE to monitor the ligand content of MPA-inhibited IMPDH samples undergoing crystallization trials, we observed that the presence of free NAD^+ and IMP "poisoned" crystal growth. Samples prepared in the absence of excess substrates (as described in the Experimental Procedures) routinely yielded well-diffracting (2.5 Å) X-ray quality crystals (Figure 6). When these same samples were titrated with NAD^+ and IMP, crystal growth was adversely affected at concentrations as low as 100 μM. Finally, crystals prepared by inhibition in the forward and reverse pathways appeared essentially identical, supporting our contention that the two pathways converge. Complete X-ray diffraction analyses are underway, and the findings of these studies will be described in a future communication.[5]

ACKNOWLEDGMENT

We gratefully acknowledge the support of all our colleagues in the Vertex IMPDH Program. In particular, we wish to thank Drs. David Armistead, Joshua Boger, Jonathan Moore, Mark Murcko, Jeffrey Saunders, and Vicki Sato for valuable discussions and critical comments on this manuscript.

REFERENCES

Allison, A. C., & Eugui, E. M. (1993) *Immunol. Rev. 136*, 5−28.
Antonino, L. C., & Wu, J. C. (1994) *Biochemistry 33*, 1753−1759.
Antonino, L. C., Straub, K., & Wu, J. C. (1994) *Biochemistry 33*, 1760−1765.
Beck, J. T., Zhao, S., & Wang, C. C. (1994) *Exp. Parasitol. 78*, 101−112.

[4] Sequence alignments suggest Cys 305 of *E. coli* IMPDH and Cys 319 in *T. foetus* IMPDH probably correspond to Cys 331 in the human and hamster IMPDH II enzymes. S. P. Chambers, unpublished, and Collart and Huberman (1988), Natsumeda *et al*. (1990), Beck *et al*. (1994), and Huete-Perez *et al*. (1995).

[5] During review of this manuscript the results of the crystallographic studies were submitted and accepted for publication [Sintchak, M. D., Fleming, M. A., Futer, O., Raybuck, S. A., Chambers, S. P., Caron, P. R., Murcko, M. A., & Wilson, K. P. (1996) *Cell* (in press)]. These studies confirm that MPA traps a covalent product of the hydride transfer reaction (IMPDH∼XMP*).

Brox, L. W., & Hampton, A. (1968) *Biochemistry 7*, 2589−2596.
Carr, S. F., Papp, E., Wu, J. C., & Natsumeda, Y. (1993) *J. Biol. Chem. 268*, 27286−27290.
Collart, F. R., & Huberman, E. (1988) *J. Biol. Chem. 263*, 15769−15772.
Collart, F. R., & Huberman, E. (1990) *Blood 75*, 570−576.
Collart, F. R., Chubb, C. B., Mirkin, B. L., & Huberman, E. (1992) *Cancer Res. 52*, 5826−5828.
Crabtree, G. W., & Henderson, J. F. (1971) *Cancer Res. 31*, 985−991.
Franklin, T. J., & Cook, J. M. (1969) *Biochem. J. 113*, 515−524.
Gilbert, H. J., Lowe, C. R., & Drabble, W. T. (1979) *Biochem. J. 183*, 481−494.
Gosio, B. (1896) *Rev. Igiene Sanita Pubbl. Ann. 7*, 825.
Hager, P. W., Collart, F. R., Huberman, E., & Mitchell, B. S. (1995) *Biochem. Pharmacol. 49*, 1323−1329.
Hedstrom, L., & Wang, C. C. (1990) *Biochemistry 29*, 849−854.
Holmes, E. W., Pehlke, D. M., & Kelley, W. N. (1974) *Biochim. Biophys. Acta 364*, 209−217.
Huete-Perez, J. A., Wu, J. C., Whitby, F. G., & Wang, C. C. (1995) *Biochemistry 34*, 13889−13894.
Hupe, D. J., Azzolina, B. A., & Behrens, N. D. (1986) *J. Biol. Chem. 261*, 8363−8369.
Ikegami, T., Natsumeda, Y., & Weber, G. (1987) *Life Sci. 40*, 2277−2282.
Jackson, R. C., Weber, G., & Morris, H. P. (1975) *Nature 256*, 330−331.
Konno, Y., Natsumeda, Y., Nagai, M., Yamaji, Y., Ohno, S., Suzuki, K., & Weber, G. (1991) *J. Biol. Chem. 266*, 506−509.
Lee, H. J., Pawlak, K., Nguyen, B. T., Robins, R. K., & Sadee, W. (1985) *Cancer Res. 45*, 5512−5520.
Link, J. O., & Straub, K. (1996) *J. Am. Chem. Soc. 118*, 2091−2092.
Nagai, M., Natsumeda, Y., Konno, Y., Hoffman, R., Irino, S., & Weber, G. (1991) *Cancer Res. 51*, 3886−3890.
Nagai, M., Natsumeda, Y., & Weber, G. (1992) *Cancer Res. 52*, 258−261.
Nakamura, H., Natsumeda, Y., Nagai, M., Takahara, J., Irino, S., & Weber, G. (1992) *Leukemia Res. 16*, 561−564.
Natsumeda, Y., Ikegami, T., Murayama, K., & Weber, G. (1988) *Cancer Res. 48*, 507−511.
Natsumeda, Y., Ohno, S., Kawasaki, H., Konno, Y., Weber, G., & Suzuki, K. (1990) *J. Biol. Chem. 265*, 5292−5295.
Nijkamp, H. J. J., & Haan, P. G. D. (1967) *Biochim. Biophys. Acta 145*, 31−40.
Okada, M., Shimura, K., Shiraki, H., & Nakagawa, H. (1983) *J. Biochem. 94*, 1605−1613.
Pichlmayr, R., & European Mycophenolate Mofetil Cooperative Study Group (1995) *Lancet 345*, 1321−1325.
Pugh, M. E., & Skibo, E. B. (1993) *Comp. Biochem. Physiol. 105B*, 381−387.
Senda, M., & Natsumeda, Y. (1994) *Life Sci. 54*, 1917−1926.
Shaw, L. M., Sollinger, H. W., Halloran, P., Morris, R. E., Yatscoff, R. W., Ransom, J., Tsina, I., Keown, P., Holt, D. W., Liberman, R., Jaklitsch, A., & Potter, J. (1995) *Ther. Drug Monit. 17*, 690−699.
Snyder, F. F., Henderson, J. F., & Cook, D. A. (1972) *Biochem. Pharmacol. 21*, 2351−2357.
Sollinger, H. W., for the U.S. Renal Transplant Mycophenolate Mofetil Study Group (1995) *Transplantation 60*, 225−232.
Tricot, G., Jayaram, H. N., Weber, G., & Hoffman, R. (1990) *Int. J. Cell Cloning 8*, 161−170.
Verham, R., Meek, T. D., Hedstrom, L., & Wang, C. C. (1987) *Mol. Biochem. Parasitol. 24*, 1−12.
Wang, W., Papov, V. V., Minakawa, N., Matsuda, A., Biemann, K., & Hedstrom, L. (1996) *Biochemistry 35*, 95−101.
Weber, G. (1983) *Cancer Res. 43*, 3466−3492.
Whitby, F. G., Huete-Perez, J., Luecke, H., & Wang, C. C. (1995) *Proteins: Struct., Funct., Genet 23*, 598−603.
Wu, J. C. (1994) *Perspect. Drug Discovery Des. 2*, 184−204.
Yamada, Y., Natsumeda, Y., & Weber, G. (1988) *Biochemistry 27*, 2193−2196.

BI9607416